Pesticides Removal Using Metal Oxide and Their Composites

Subjects: Chemistry, Applied

Contributor: Haneen H. Shanaah , Eman F. H. Alzaimoor , Suad Rashdan , Amina A. Abdalhafith , Ayman H. Kamel

Persistent organic chemicals (POPs) are highly hazardous to the ecosystem and living organisms. Their non-biodegradability allows them to accumulate easily in the food chain, affecting both humans and wildlife. Pesticides are one class of POPs with half-lives that can extend to years. They have been used abundantly to control the growth of the crops by exterminating pests including insects, fungi, and microorganisms in agricultural farms.

metal oxide nanomaterials organic pesticides photocatalysis

1. Classification of Pesticides

The demand for categorizing pesticides has been raised significantly because of the increased number of pesticides, along with the variation in physical and chemical properties [1]. A considerable volume of literature has been published in this field. Recently, scientists classified pesticides based on origin and on target. Pesticides generally originate from organic, inorganic, and biological sources [2]. **Table 1** elaborates on the organic class of pesticides. The pesticides' chemical structures are shown in **Figure 1**.

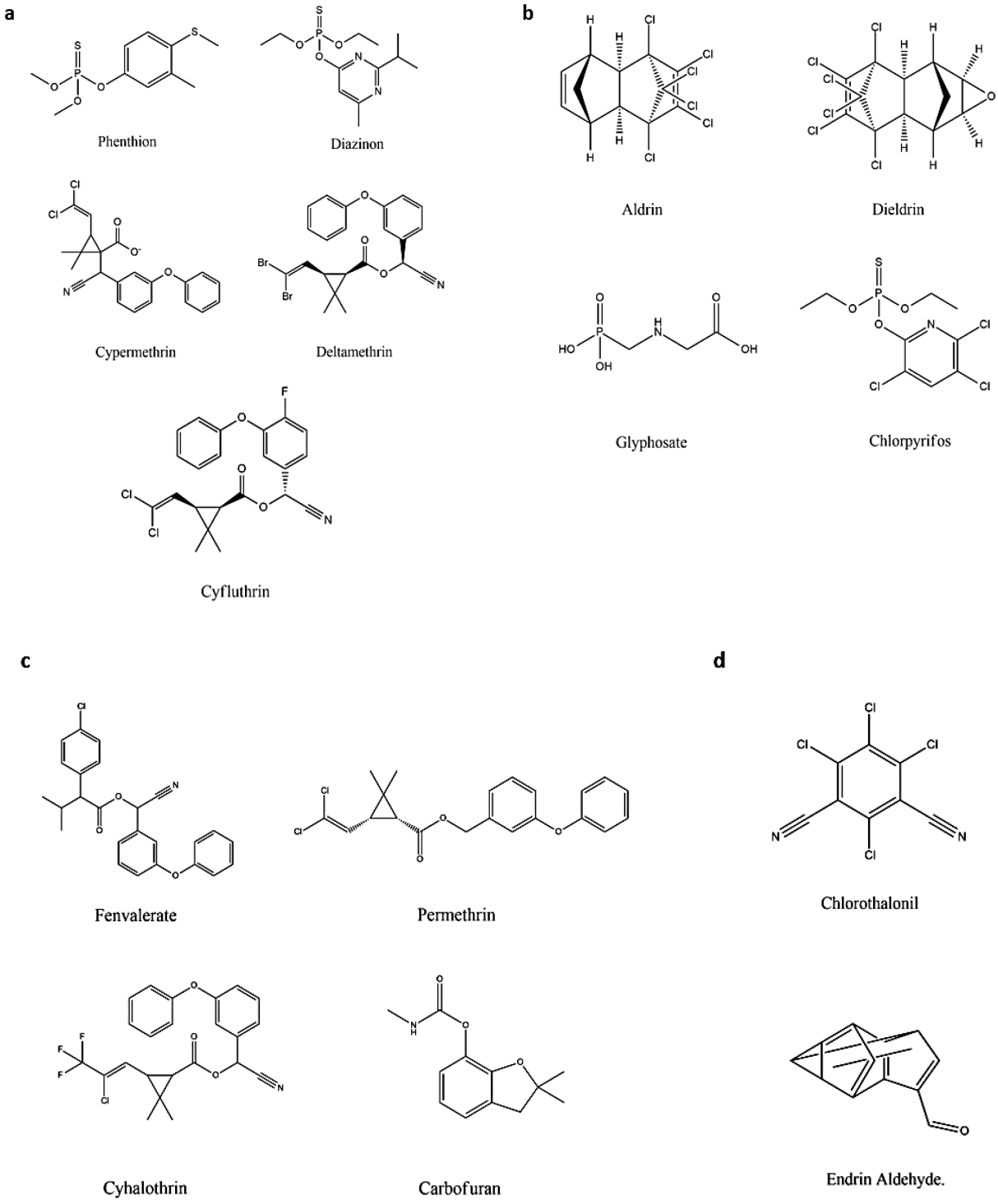

Figure 1. The chemical structures of some pesticides: (**a**) Pyrethroids, (**b**) Organophosphates, (**c**) Carbamates, and (**d**) Organochlorines.

Table 1. Classification of organic pesticides based on origin.

Origin	Source	Class	Example	Features	Refs.
Organic	Natural	Plants Phytochemicals	Essential oil, plant extracts, and	Low Toxicity, limited persistence in the environment, and complicated	[3][4]

Origin	Source	Class	Example	Features	Refs.
			leftover oilseed cakes.	structures that prevent resistance in pests.	
	Synthetic	Pyrethroids	Phenthion, Diazinon, Cypermethrin, Deltamethrin, Cyfluthrin, and Cypermethrin	Effect the sodium channel in insects, resulting in paralysis of the organism; highly toxic to insects and fish but less to mammals; unstable upon the exposure of light; and commonly used in food.	[5][6] [7][8]
		Organophosphates	Aldrin, Dieldrin, Glyphosate, and Chlorpyrifos.	Cause paralysis, resulting in death, and dominant for variety of pests.	[9] [10]
		Carbamates	Fenvalerate, Permethrin, Cyhalothrin, and Carbofuran.	Effect the nerve system of the pests, resulting in poisoning and death, and low pollution is caused upon degradation.	[11] [12] [13] [14]
		Organochlorine	Chlorothalonil and Endrin Aldehyde.	Used for insects, long persistent in environment, affecting the nerve system and causing paralysis and death of the pests.	

2. Removal of Pesticides Using Functionalized Metal Oxide Nanomaterials by Adsorption

The hazards and consequences resulting from the massive use of pesticides raised the demand for efficient techniques to be employed for the removal of these contaminants. The adsorption technique has gained popularity as a simple, effective, insensitive, and flexible method [15]. It is a physiochemical method that occurs mostly in the solid–liquid form, though liquid–liquid and liquid–gas forms are also known [16][17][18].

In adsorption, the molecules of liquid or gases are bound to the surface of the solid. The material that provides the surface is called the adsorbent. The contaminants in the liquid or the gaseous phase are called adsorbates. Among the adsorbents reported in the literature, metal oxides have been proven as excellent adsorbents for the remediation of pesticides because of the large surface area provided for the adsorption of the pollutant [19]. The active sites and the functional groups, such as -OH, -COOH, and -C=OH, have a great impact on the efficiency of the adsorption process [20][21]. Moreover, metal oxides, having porous structures, thermal stability, low toxicity, and easy recovery, are all important for a good adsorbent. Two types of interaction between the adsorbent and the adsorbate are present: chemisorption and physisorption. Chemisorption is basically a chemical reaction between the adsorbent and the adsorbate, and it is an irreversible process. It is controlled by chemical bonds such as covalent, chelation, complex formation, proton displacement, and redox-reactions. On the other hand, physisorption, which is more dominant, is a reversible process controlled by Van der Wal's bonds, dipole–dipole attraction, and London force, etc. [22].

The adsorption process depends on various parameters that need to be optimized, including pH, temperature, time, concentration of contaminant, and sorbent dosage. **Table 2** represents the adsorption capacity Q_{max} (mg/g) and the percentage removal of targeted pesticides using metal oxide nanoparticles at different parameters. The adsorption capacity is calculated in (mg/g) using the formula in Equation (1):

$$Q_{max} = \frac{C_o - C_e}{m} \times V \quad (1)$$

where C_o is the initial concentration of the pesticide (mg/L), C_e is the pesticide concentration at equilibrium (mg/L), m is the mass of adsorbent (g), and V is the volume of the solution (L).

The adsorption isotherm and the adsorption kinetics are used to elucidate the adsorption process and to indicate the type of mechanism. The adsorption isotherm is expressed by Langmuir, Freundlich, Sips, Temkin, Redlich Peterson, Henry, and Dubinin–Astakhov (DA) models. Langmuir, Freundlich, and Dubinin–Astakhov models are most frequently used. Langmuir isotherm investigates a monolayer adsorption onto a homogeneous adsorbent, whereas Freundlich illustrates a multilayer adsorption onto a heterogeneous adsorbent. The Dubinin–Astakhov model is used to calculate the mean free adsorption energy E (J/mol). The physisorption mechanism gives an E value smaller than 8 J/mol. However, values of E from 16 J/mol to 40 J/mol indicate a chemisorption mechanism. The adsorption kinetics are equations that indicate the type of interactions between the adsorbent and the adsorbate (contaminant). Chemisorption interaction is described by a pseudo-second-order equation. The pseudo-first-order equation is applied for the physisorption interaction [23][24].

Despite the advantages of adsorption, there is one certain drawback associated with the use of this technique: it produces secondary pollutants which require highly advanced procedures for recycling and decomposing for them to be used in the industrial field [25].

Table 2. Adsorptive remediation of pesticides using metal oxides NPs.

Adsorbent [a]	Targeted Pesticides [b]	Target Operation Parameters					Adsorption Modelling				Ref.
		Pesticide Conc.	Adsorbent Dosage (g) or g/L	pH	Temp. (K)	Time (min)	Kinetics [c]	Isotherm [d]	Mechanism [e]	Q_{max} (mg/g) or Percentage Removal (%)/Percentage Recovery	
Co_3O_4/G-MCM-41	Methyl parathion	-	-	-	-	-	PFO, PSO	L, F, DA	-	175.2	[26]
NiO/Co@C	Chlorothalonil	0.045 g/L	0.01 g	-	-	15	PSO	L	π-CM, H	62.2	[27]
	Tebuconazole	0.045 g/L	0.01 g	-	-	15	PSO	L	π-CM, H	40.5	

Adsorbent [a]	Targeted Pesticides [b]	Target Operation Parameters					Adsorption Modelling				Ref.
		Pesticide Conc.	Adsorbent Dosage (g) or g/L	pH	Temp. (K)	Time (min)	Kinetics [c]	Isotherm [d]	Mechanism [e]	Q_{max} (mg/g) or Percentage Removal (%)/Percentage Recovery	
	Chlorpyrifos	0.045 g/L	0.01 g	-	-	15	PSO	L	π-CM, H	60.3	
	Butralin	0.045 g/L	0.01 g	-	-	15	PSO	L	π-CM, H	50.2	
	Deltamethrin	0.045 g/L	0.01 g	-	-	15	PSO	L	π-CM, H	54.1	
	Pyridaben	0.045 g/L	0.01 g	-	-	15	PSO	L	π-CM, H	51.3	
CeO_2	2,4-Dichlorophenoxyacetic acid	0.01 g/L	0.025 g	-	308	120	PSO	L, F, S	π–π, e^-	95.78	[28]
Fe_3O_4@ZnAl-LDH@MIL-53(Al)	Triadimefon	5.0–600 mg kg^{-1}	30 g/L	6	308.15	5	PSO	L	π–π, H, C, (π-CM), P	46.08	[29]
$MgFe_2O_4$	Chlorpyrifos	20 mg/L	0.01 g/L	10	295	360	PSO	L	-	4461	[30]
Fe_3O_4	Atrazine	50 mg/L	0.1 g	2	298	55	PFO	L	-	77.5	[31]
	Methoxychlor	50 mg/L	0.1 g	2	298	55	PFO	L	-	163.9	
ZnO	Naphthalene	25 mg/L	0.012 g	4	298	40	PSO	L, F, T	-	66.8	
CTAB-ZnO	Naphthalene	25 mg/L	0.08 g	4	298	40	PSO	L, F, T	-	89.96	[32]
BMTF-IL-ZnO	Naphthalene	25 mg/L	0.06 g	4	298	40	PSO	L, F, T	-	148.3	
$ZnO/ZnFe_2O_4$	Atrazine	50 mL aq. solution	0.4 g/L	7	298	4320	-	D.A	π–π, H, h, e-	-	[33]
Fe_3O_4@SiO_2@GO-2-phenylethylamine	Chlorpyrifos	10 mL aq. Solution	0.015 g	7	298	15	PSO	S	π–π, H	88%	[34]
	Malathion	10 mL aq. Solution	0.015 g	7	298	15	PSO	S	H	76%	
	Parathion	10 mL aq.	0.015 g	7	298	15	PSO	S	π–π, H	85%	

Adsorbent [a]	Targeted Pesticides [b]	Target Operation Parameters					Adsorption Modelling				Ref.
		Pesticide Conc.	Adsorbent Dosage (g) or g/L	pH	Temp. (K)	Time (min)	Kinetics [c]	Isotherm [d]	Mechanism [e]	Q_{max} (mg/g) or Percentage Removal (%)/Percentage Recovery	
		Solution									
Fe_3O_4/MOF-99	Dinotefuran	0.3–1.5 ng/mL	0.015 g	-	-	20	-	-	π–π	88–107%	[35]
	Thiamethoxam	0.3–1.5 ng/mL	0.015 g	-	-	20	-	-	π–π	88–107%	
Fe_3O_4@SiO_2@MOF/TiO_2	Triadimenol	0.001 g/L	0.04 g	7	298–313.15	1–60	PSO	-	π–π	90.2–104%	[36]
	Hexaconazole	0.001 g/L	0.04 g	7	298–313.15	1–60	PSO	-	π–π	90.2–104%	
	Diniconazole	0.001 g/L	0.04 g	7	298–313.15	1–60	PSO	-	π–π	90.2–104%	
Fe_3O_4-GO@MOF-199.	Flusilazole	0.002 g/L	0.02 g	-	-	15	-	-	h, π–π, H, e^-	0.0356	[37]
	Fenbuconazole	0.002 g/L	0.02 g	-	-	15	-	-	h, π–π, H, e^-	0.0342	
	Myclobutanil	0.002 g/L	0.02 g	-	-	15	-	-	h, π–π, H, e^-	0.0324	
Fe_3O_4–MWCNTs-ZIF-8	Triazophos	0.015 g	0.002–0.08 g/L	4	RT	15	-	F	-	3.12	[38]
	Diazinon	0.015 g	0.002–0.08 g/L	4	RT	15	-	F	-	2.59	
	Phosalone	0.015 g	0.002–0.08 g/L	4	RT	15	-	F	-	3.80	
	Profenofos	0.015 g	0.002–0.08 g/L	4	RT	15	-	F	-	3.89	
	Methidathion	0.015 g	0.002–0.08 g/L	4	RT	15	-	F	-	2.34	
	Ethoprop	0.015 g	0.002–0.08 g/L	4	RT	15	-	F	-	2.18	
	Sulfotep	0.015 g	0.002–0.08 g/L	4	RT	15	-	F	-	2.84	

3. Removal of Pesticides Using Functionalized Metal Oxide Nanomaterials by Photocatalytic Degradation

Photocatalytic degradation is an advanced oxidation process that destroys toxic substances into other harmless products. Unlike other remediation techniques, photocatalytic degradation completely mineralizes the toxicant, without the production of secondary waste [50]. The mechanism of photocatalytic degradation starts when the photocatalyst is irradiated under UV or visible light that has energy equal to or greater than its band gap [51]. The detailed mechanism of the reaction is shown in Equation (2) to Equation (8). Notably, photocatalytic degradation of

Adsorbent [a]	Targeted Pesticides [b]	Target Operation Parameters					Adsorption Modelling				Ref.
		Pesticide Conc.	Adsorbent Dosage (g) or g/L	pH	Temp. (K)	Time (min)	Kinetics [c]	Isotherm [d]	Mechanism [e]	Q_{max} (mg/g) or Percentage Removal (%)/Percentage Recovery	
Chitosan–CuO	Isazofos	0.015 g	0.002–0.08 g/L	4	RT	15	-	F	-	3	[39]
	Thiophanate-methyl	0.1 g/L	0.1 g	7	RT	25	-	L, F	h	250	
	Methomyl	0.1 g/L	0.1 g	7	RT	25	-	L.F	-	20	
	Malathion	0.02 g/L	1 g/L	2	303	960	PSO	L, F	-	322.6	
Chitosan-ZnO	Thiophanate-methyl	0.1 g/L	0.1 g	7	RT	25	-	L, F	h	100	
	Methomyl	0.1 g/L	0.1 g	7	RT	25	-	L, F	-	10	
	Permethrin	0.0001 g/L	0.5 g	7	298	90	-	-	-	99%	[40]
Fe_3O_4/CuO/Activa-ted carbon	Imidacloprid	0.01 g/L	0.02 g	7	298	10	PSO	F	C	99%	[41]
ZnO-IPPs	Chlorpyrifos	0.01–0.6 g/L	0.03 g	2	303–323	30	PSO	L, F, T, D. A	-	47.846	[42]
ZnO-CP	Metribuzin	0.033–0.155	0.08 g	3	303–363	80	PSO	F	-	200	[43]
MOM-Fe_3O_4	Triclosan	0.005–0.2 g/L	0.01–0.05 g/L	4, 7, 10	293, 303, 313	600	PFO	L	-	103.45	[44]
N-NiO@N-Fe_3O_4@N-ZnO	Atrazine	0.04 g/L	0.1 g	5	-	80	PSO	L	-	92%	[45]
$MgAl_2O_4$	Dimethomorph	-	0.5–2 g	5.5	-	10	-	-	-	% Recovery = 90–94%	[46]
Fe_3O_4 @PS	Lindane	2, 10, 50, 200 µg/L	0.02 g/L	-	RT	<20	PSO	L	-	10.2	[47]
	Aldrin	2, 10, 50, 200 µg/L	0.02 g/L	-	RT	<20	PSO	L	-	24.7	
	Dieldrin	2, 10, 50, 200	2×10^{-5} g/L	-	RT	<20	PSO	L	-	21.3	

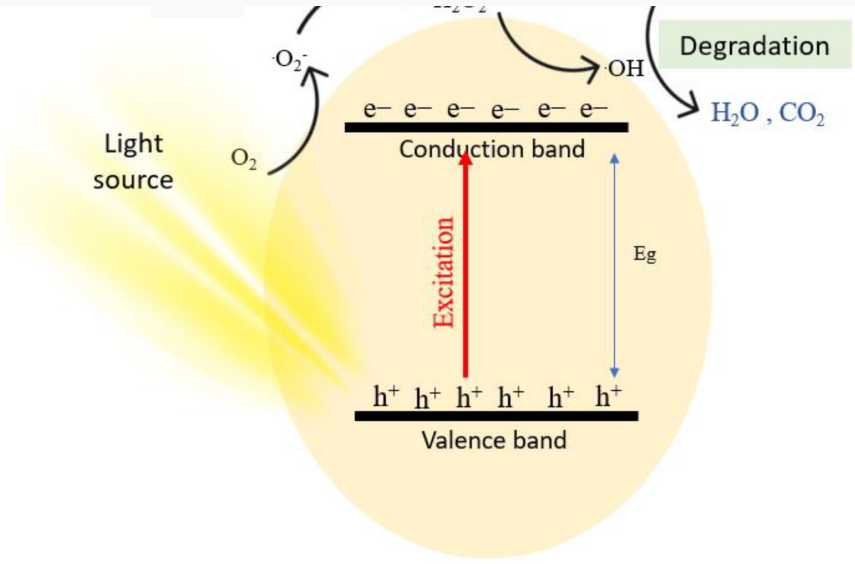

Figure 2. A schematic mechanism for the photodegradation of a pesticide.

Adsorbent [a]	Targeted Pesticides [b]	Target Operation Parameters					Adsorption Modelling				Ref.
		Pesticide Conc.	Adsorbent Dosage (g) or g/L	pH	Temp. (K)	Time (min)	Kinetics [c]	Isotherm [d]	Mechanism [e]	Q_{max} (mg/g) or Percentage Removal (%)/Percentage Recovery	
		µg/L									
MgO	Endrin	2, 10, 50, 200 µg/L	2 × 10^{-5} g/L	-	RT	<20	PSO	L	-	33.5	[54]
MgO	Diazinon	0.30 g/L	0.05 or 0.10 g	-	-	<5	-	-	-	21–37%	[48]
MgO	Fenitrothion	0.28 g/L	0.05 or 0.10 g	-	-	5–60	-	-		27–47%	[55]
$Fe_3O_4@nSiO_2@mSiO_2$	DDT	0.0015 g/L	0.05 g	-	-	15	PSO	-	-	94%	[49]

RT = room temperature; [a] Adsorbent: ZnONPs-IPPs = zinc oxide nanoparticles-impregnated pea peels; MOM-Fe_3O_4 = functionalized iron oxide nanoparticles with Moringa oleifera Lam. seeds; Fe_3O_4 @PS = magnetic nanosphere coated by polystyrene; ZnO-CP = zinc oxide with cucumber peel; CTAB-ZnO = cetyltrimethylammonium bromide functionalized zinc oxide; BMTF-IL-ZnO = 1-Butyl-3-methylimidazolium tetrafluoroborate functionalized zinc oxide; Hr-MgO = hierarchical magnesium oxide; [b] targeted pesticides fenitrothion = dimethoxy-(3-methyl-4-nitrophenoxy)-thioxophosphorane; DDT = dichloro-diphenyl-trichloroethane; Diazinone = diethoxy-[(2-isopropyl-6- methyl-4-pyrimidinyl)oxy]-thioxophosphorane; [c] Kinetic equation; PSO = pseudo-second order; PFO = pseudo-first order; [d] Isotherm equation; L = Langmuir; F = Freundlich; S = Sips; T = Temkin; DA = Dubinin–Astakhov; [e] Mechanisms: electrostatic interaction (e^-), hydrophobic interaction (h), π–π interaction (π–π), π-complex formation with cations (including metal or positive ion charge groups) (π-CM), hydrogen bond interaction (H), coordination or covalent bond (C).

…iency of …tal oxide …naximum

Several parameter… …e and type of …on time. …process. …a result …airs and, consequently, more hydroxyl radicals. However, it is worth mentioning that after very high dosages of the photocatalyst, the efficiency of the reaction decreases due to the blockage of light penetration [56]. Concerning the concentration of the pesticide, at high dosages of the pollutant, most studies reported a decrease in the efficiency of degradation, as reported in **Table 2**. Increasing the dosage of the pesticide allows for the adsorption of the pesticide on the active sites of the catalyst, preventing the generation of hydroxyl radicals [57]. Depending on the structure of both pesticide and the nano-photocatalyst, the pH can affect the reaction behavior between them. The reaction will be favorable in the pH that allows for the attraction of the photocatalyst and the pesticide, as well as the accelerated production of hydroxyl radicals [58]. The effect of irradiation time is directly proportional to the efficiency of degradation. The increase of irradiation time permits more excitation to occur, and consequently, more radicals are formed [59].

Metal oxide semiconductors, such as ZnO and TiO_2 nanomaterials, are the most appropriate for photocatalytic degradation (**Table 2**) [53]. This is attributed to the fact that they can produce electron/hole pairs (e^-/h^+) more when irradiated with light. Most photocatalysis research focuses on TiO_2 nanomaterials [60][61][62]. The problem with ZnO NPs is the fast recombination of the generated electron/holes [57]. However, recently, it has been discovered that doping the semiconductors with other metals, or further functionalizing them, leads to better separation of charges [63].

References

1. Hassaan, M.A.; El Nemr, A. Pesticides pollution: Classifications, human health impact, extraction and treatment techniques. Egypt. J. Aquat. Res. 2020, 46, 207–220.

2. Abubakar, Y.; Tijjani, H.; Egbuna, C.; Adetunji, C.O.; Kala, S.; Kryeziu, T.L.; Ifemeje, J.C.; Patrick-Iwuanyanwu, K.C. Chapter 3—Pesticides, History, and Classification. In Natural Remedies for Pest, Disease and Weed Control; Egbuna, C., Sawicka, B., Eds.; Academic Press: Cambridge, MA, USA, 2020; pp. 29–42.

3. Sousa, R.M.O.F.; Cunha, A.C.; Fernandes-Ferreira, M. The potential of Apiaceae species as sources of singular phytochemicals and plant-based pesticides. Phytochemistry 2021, 187,

112714.

4. George, D.; Finn, R.; Graham, K.; Sparagano, O. Present and future potential of plant-derived products to control arthropods of veterinary and medical significance. Parasites Vectors 2014, 7, 28.
5. Quijano, L.; Yusà, V.; Font, G.; Pardo, O. Chronic cumulative risk assessment of the exposure to organophosphorus, carbamate and pyrethroid and pyrethrin pesticides through fruit and vegetables consumption in the region of Valencia (Spain). Food Chem. Toxicol. 2016, 89, 39–46.
6. Pirsaheb, M.; Fattahi, N.; Rahimi, R.; Sharafi, K.; Ghaffari, H.R. Evaluation of abamectin, diazinon and chlorpyrifos pesticide residues in apple product of Mahabad region gardens: Iran in 2014. Food Chem. 2017, 231, 148–155.
7. Blankson, G.K.; Osei-Fosu, P.; Adeendze, E.A.; Ashie, D. Contamination levels of organophosphorus and synthetic pyrethroid pesticides in vegetables marketed in Accra, Ghana. Food Control 2016, 68, 174–180.
8. Yuan, Y.; Chen, C.; Zheng, C.; Wang, X.; Yang, G.; Wang, Q.; Zhang, Z. Residue of chlorpyrifos and cypermethrin in vegetables and probabilistic exposure assessment for consumers in Zhejiang Province, China. Food Control 2014, 36, 63–68.
9. Ciasca, B.; Pecorelli, I.; Lepore, L.; Paoloni, A.; Catucci, L.; Pascale, M.; Lattanzio, V.M.T. Rapid and reliable detection of glyphosate in pome fruits, berries, pulses and cereals by flow injection—Mass spectrometry. Food Chem. 2020, 310, 125813.
10. Mojsak, P.; Łozowicka, B.; Kaczyński, P. Estimating acute and chronic exposure of children and adults to chlorpyrifos in fruit and vegetables based on the new, lower toxicology data. Ecotoxicol. Environ. Saf. 2018, 159, 182–189.
11. Li, Z.; Zhang, Y.; Zhao, Q.; Wang, C.; Cui, Y.; Li, J.; Chen, A.; Liang, G.; Jiao, B. Occurrence, temporal variation, quality and safety assessment of pesticide residues on citrus fruits in China. Chemosphere 2020, 258, 127381.
12. Hirano, T.; Suzuki, N.; Ikenaka, Y.; Hoshi, N.; Tabuchi, Y. Neurotoxicity of a pyrethroid pesticide deltamethrin is associated with the imbalance in proteolytic systems caused by mitophagy activation and proteasome inhibition. Toxicol. Appl. Pharmacol. 2021, 430, 115723.
13. Nurdin, M.; Maulidiyah, M.; Salim, L.O.A.; Muzakkar, M.Z.; Umar, A.A. High performance cypermethrin pesticide detection using anatase TiO2-carbon paste nanocomposites electrode. Microchem. J. 2019, 145, 756–761.
14. Xia, Y.; Bian, Q.; Xu, L.; Cheng, S.; Song, L.; Liu, J.; Wu, W.; Wang, S.; Wang, X. Genotoxic effects on human spermatozoa among pesticide factory workers exposed to fenvalerate. Toxicology 2004, 203, 49–60.

15. Gupta, D.; Jamwal, D.; Rana, D.; Katoch, A. 26—Microwave synthesized nanocomposites for enhancing oral bioavailability of drugs. In Applications of Nanocomposite Materials in Drug Delivery; Inamuddin, A.M.A., Mohammad, A., Eds.; Woodhead Publishing: Cambridge, UK, 2018; pp. 619–632.
16. Dabrowski, A. Adsorption--from theory to practice. Adv Colloid Interface Sci 2001, 93, 135–224.
17. del Mar Orta, M.; Martín, J.; Medina-Carrasco, S.; Santos, J.L.; Aparicio, I.; Alonso, E. Adsorption of propranolol onto montmorillonite: Kinetic, isotherm and pH studies. Appl. Clay Sci. 2019, 173, 107–114.
18. Derylo-Marczewska, A.; Blachnio, M.; Marczewski, A.W.; Swiatkowski, A.; Buczek, B. Adsorption of chlorophenoxy pesticides on activated carbon with gradually removed external particle layers. Chem. Eng. J. 2017, 308, 408–418.
19. Sharma, L.; Kakkar, R. Hierarchically structured magnesium based oxides: Synthesis strategies and applications in organic pollutant remediation. CrystEngComm 2017, 19, 6913–6926.
20. Batzill, M. Fundamental aspects of surface engineering of transition metal oxide photocatalysts. Energy Environ. Sci. 2011, 4, 3275–3286.
21. Mahmoud, A.M.; Ibrahim, F.A.; Shaban, S.A.; Youssef, N.A. Adsorption of heavy metal ion from aqueous solution by nickel oxide nano catalyst prepared by different methods. Egypt. J. Pet. 2015, 24, 27–35.
22. Crini, G.; Lichtfouse, E.; Wilson, L.D.; Morin-Crini, N. Adsorption-Oriented Processes Using Conventional and Non-conventional Adsorbents for Wastewater Treatment. In Green Adsorbents for Pollutant Removal: Fundamentals and Design; Crini, G., Lichtfouse, E., Eds.; Springer International Publishing: Cham, Switzerland, 2018; pp. 23–71.
23. Edet, U.A.; Ifelebuegu, A.O. Kinetics, Isotherms, and Thermodynamic Modeling of the Adsorption of Phosphates from Model Wastewater Using Recycled Brick Waste. Processes 2020, 8, 665.
24. Ahmed, M.J.; Hameed, B.H. Insights into the isotherm and kinetic models for the coadsorption of pharmaceuticals in the absence and presence of metal ions: A review. J. Environ. Manag. 2019, 252, 109617.
25. Gusain, R.; Gupta, K.; Joshi, P.; Khatri, O.P. Adsorptive removal and photocatalytic degradation of organic pollutants using metal oxides and their composites: A comprehensive review. Adv. Colloid Interface Sci. 2019, 272, 102009.
26. Adeola, A.O.; Abiodun, B.A.; Adenuga, D.O.; Nomngongo, P.N. Adsorptive and photocatalytic remediation of hazardous organic chemical pollutants in aqueous medium: A review. J. Contam. Hydrol. 2022, 248, 104019.

27. Salam, M.A.; AbuKhadra, M.R.; Mohamed, A.S. Effective oxidation of methyl parathion pesticide in water over recycled glass based-MCM-41 decorated by green Co3O4 nanoparticles. Environ. Pollut. 2020, 259, 113874.
28. Zhao, J.; Huang, P.; Wang, X.; Yang, J.; Zhou, Z.; Du, X.; Lu, X. Efficient adsorption removal of organic nitrogen pesticides: Insight into a new hollow NiO/ magnetic nanocomposites derived from metal-organic framework. Sep. Purif. Technol. 2022, 287, 120608.
29. Abdelillah Ali Elhussein, E.; Şahin, S.; Bayazit, Ş.S. Preparation of CeO2 nanofibers derived from Ce-BTC metal-organic frameworks and its application on pesticide adsorption. J. Mol. Liq. 2018, 255, 10–17.
30. Zhou, D.-D.; Lu, Z.-H.; Chen, M.; Zhuang, L.-Y.; Cao, Y.-W.; Liu, X.; Senosy, I.A.; Yang, Z.-H. A novel magnetic double MOF composite is synthesized for removing azole fungicides economically and efficiently. Appl. Surf. Sci. 2022, 594, 153441.
31. Sharma, L.; Kakkar, R. Magnetically retrievable one-pot fabrication of mesoporous magnesium ferrite (MgFe2O4) for the remediation of chlorpyrifos and real pesticide wastewater. J. Environ. Chem. Eng. 2018, 6, 6891–6903.
32. Nayak, A.; Bhushan, B.; Sharma, P.K.; Gupta, V. Development of Magnetic Nanoparticles from Poplar Sawdust for Removal of Pesticides from Aqueous Solution. J. Graph. Era Univ. 2018, 6, 55–70.
33. Kaur, Y.; Bhatia, Y.; Chaudhary, S.; Chaudhary, G.R. Comparative performance of bare and functionalize ZnO nanoadsorbents for pesticide removal from aqueous solution. J. Mol. Liq. 2017, 234, 94–103.
34. Wanjeri, V.W.O.; Sheppard, C.J.; Prinsloo, A.R.E.; Ngila, J.C.; Ndungu, P.G. Isotherm and kinetic investigations on the adsorption of organophosphorus pesticides on graphene oxide based silica coated magnetic nanoparticles functionalized with 2-phenylethylamine. J. Environ. Chem. Eng. 2018, 6, 1333–1346.
35. Chen, D.; Chen, C.; Shen, W.; Quan, H.; Chen, S.; Xie, S.; Luo, X.; Guo, L. MOF-derived magnetic porous carbon-based sorbent: Synthesis, characterization, and adsorption behavior of organic micropollutants. Adv. Powder Technol. 2017, 28, 1769–1779.
36. Cao, X.; Liu, G.; She, Y.; Jiang, Z.; Jin, F.; Jin, M.; Du, P.; Zhao, F.; Zhang, Y.; Wang, J. Preparation of magnetic metal organic framework composites for the extraction of neonicotinoid insecticides from environmental water samples. RSC Adv. 2016, 6, 113144–113151.
37. Su, H.; Lin, Y.; Wang, Z.; Wong, Y.L.; Chen, X.; Chan, T.W. Magnetic metal-organic framework-titanium dioxide nanocomposite as adsorbent in the magnetic solid-phase extraction of fungicides from environmental water samples. J. Chromatogr. A 2016, 1466, 21–28.

38. Liu, G.; Li, L.; Huang, X.; Zheng, S.; Xu, D.; Xu, X.; Zhang, Y.; Lin, H. Determination of triazole pesticides in aqueous solution based on magnetic graphene oxide functionalized MOF-199 as solid phase extraction sorbents. Microporous Mesoporous Mater. 2018, 270, 258–264.
39. Liu, G.; Li, L.; Huang, X.; Zheng, S.; Xu, X.; Liu, Z.; Zhang, Y.; Wang, J.; Lin, H.; Xu, D. Adsorption and removal of organophosphorus pesticides from environmental water and soil samples by using magnetic multi-walled carbon nanotubes @ organic framework ZIF-8. J. Mater. Sci. 2018, 53, 10772–10783.
40. Badawy, M.E.I.; El-Nouby, M.A.M.; Marei, A.E.-S.M. Development of a Solid-Phase Extraction (SPE) Cartridge Based on Chitosan-Metal Oxide Nanoparticles (Ch-MO NPs) for Extraction of Pesticides from Water and Determination by HPLC. Int. J. Anal. Chem. 2018, 2018, 3640691.
41. Moradi Dehaghi, S.; Rahmanifar, B.; Moradi, A.M.; Azar, P.A. Removal of permethrin pesticide from water by chitosan–zinc oxide nanoparticles composite as an adsorbent. J. Saudi Chem. Soc. 2014, 18, 348–355.
42. Parsaie, A.; Rahbar, N.; Baezat, M. A New Fe3O4/CuO/AC Nanocomposite for Imidacloprid Removal: Characterization, Optimization, and Adsorption Modeling. Res. Sq. 2021.
43. ul Haq, A.; Saeed, M.; Usman, M.; Naqvi, S.A.R.; Bokhari, T.H.; Maqbool, T.; Ghaus, H.; Tahir, T.; Khalid, H. Sorption of chlorpyrifos onto zinc oxide nanoparticles impregnated Pea peels (Pisum sativum L): Equilibrium, kinetic and thermodynamic studies. Environ. Technol. Innov. 2020, 17, 100516.
44. Haq, A.; Saeed, M.; Muneer, M.; Jamal, M.; Maqbool, T.; Tahir, T. Biosorption of metribuzin pesticide by Cucumber (Cucumis sativus) peels-zinc oxide nanoparticles composite. Sci. Rep. 2022, 12, 5840.
45. Cusioli, L.F.; Quesada, H.B.; Barbosa de Andrade, M.; Gomes, R.G.; Bergamasco, R. Application of a novel low-cost adsorbent functioned with iron oxide nanoparticles for the removal of triclosan present in contaminated water. Microporous Mesoporous Mater. 2021, 325, 111328.
46. Allam, E.A.; Ali, A.S.M.; Elsharkawy, R.M.; Mahmoud, M.E. Framework of nano metal oxides 3O4@N-ZnO for adsorptive removal of atrazine and bisphenol-A from wastewater: Kinetic and adsorption studies. Environ. Nanotechnol. Monit. Manag. 2021, 16, 100481.
47. Rao, T.N.; Balaji, A.P.B.; Panagal, M.; Parvatamma, B.; Selvaraj, B.; Panneerselvam, S.; Aruni, W.; Subramanian, K.; Sampath Renuga, P.; Pandian, S. Nanoremediation of dimethomorph in water samples using magnesium aluminate nanoparticles. Environ. Technol. Innov. 2020, 20, 101176.
48. Lan, J.; Cheng, Y.; Zhao, Z. Effective organochlorine pesticides removal from aqueous systems by magnetic nanospheres coated with polystyrene. J. Wuhan Univ. Technol.-Mater. Sci. Ed. 2014, 29, 168–173.

49. Armaghan, M.; Amini, M.M. Adsorption of diazinon and fenitrothion on nanocrystalline magnesium oxides. Arab. J. Chem. 2017, 10, 91–99.
50. Shirzad-Siboni, M.; Jonidi-Jafari, A.; Farzadkia, M.; Esrafili, A.; Gholami, M. Enhancement of photocatalytic activity of Cu-doped ZnO nanorods for the degradation of an insecticide: Kinetics and reaction pathways. J. Environ. Manag. 2017, 186, 1–11.
51. Liu, F.; Tian, H.; He, J. Adsorptive performance and catalytic activity of superparamagnetic @mSiO2 core–shell microspheres towards DDT. J. Colloid Interface Sci. 2014, 419, 68–72.
52. Qumar, U.; Hassan, J.Z.; Bhatti, R.A.; Raza, A.; Nazir, G.; Nabgan, W.; Ikram, M. Photocatalysis vs adsorption by metal oxide nanoparticles. J. Mater. Sci. Technol. 2022, 131, 122–166.
53. Vaya, D.; Surolia, P.K. Semiconductor based photocatalytic degradation of pesticides: An overview. Environ. Technol. Innov. 2020, 20, 101128.
54. Gaya, U.I.; Abdullah, A.H. Heterogeneous photocatalytic degradation of organic contaminants over titanium dioxide: A review of fundamentals, progress and problems. J. Photochem. Photobiol. C Photochem. Rev. 2008, 9, 1–12.
55. Krishnasamy, L.; Krishna, K.; Subpiramaniyam, S. Photocatalytic Degradation of Atrazine in Aqueous Solution Using La-Doped ZnO/PAN Nanofibers. Environ. Sci. Pollut. Res. 2022, 29, 54282–54291.
56. Rani, M.; Yadav, J.; Keshu; Shanker, U. Green synthesis of sunlight responsive zinc oxide coupled cadmium sulfide nanostructures for efficient photodegradation of pesticides. J. Colloid Interface Sci. 2021, 601, 689–703.
57. Zhu, Z.; Guo, F.; Xu, Z.; Di, X.; Zhang, Q. Photocatalytic degradation of an organophosphorus pesticide using a ZnO/rGO composite. RSC Adv. 2020, 10, 11929–11938.
58. Anirudhan, T.S.; Shainy, F.; Sekhar, V.C.; Athira, V.S. Highly efficient photocatalytic degradation of chlorpyrifos in aqueous solutions by nano hydroxyapatite modified CFGO/ZnO nanorod composite. J. Photochem. Photobiol. A Chem. 2021, 418, 113333.
59. Soltani-nezhad, F.; Saljooqi, A.; Shamspur, T.; Mostafavi, A. Photocatalytic degradation of imidacloprid using GO/Fe3O4/TiO2-NiO under visible radiation: Optimization by response level method. Polyhedron 2019, 165, 188–196.
60. Zangiabadi, M.; Shamspur, T.; Saljooqi, A.; Mostafavi, A. Evaluating the efficiency of the GO-Fe3O4/TiO2 mesoporous photocatalyst for degradation of chlorpyrifos pesticide under visible light irradiation. Appl. Organomet. Chem. 2019, 33, e4813.
61. Andronic, L.; Vladescu, A.; Enesca, A. Synthesis, Characterisation, Photocatalytic Activity, and Aquatic Toxicity Evaluation of TiO2 Nanoparticles. Nanomaterials 2021, 11, 3197.

62. Čižmar, T.; Panžić, I.; Capan, I.; Gajović, A. Nanostructured TiO2 photocatalyst modified with Cu for improved imidacloprid degradation. Appl. Surf. Sci. 2021, 569, 151026.
63. Khan, S.H.; Pathak, B. Zinc oxide based photocatalytic degradation of persistent pesticides: A comprehensive review. Environ. Nanotechnol. Monit. Manag. 2020, 13, 100290.